IJEEC

International Journal of Electrical Engineering and Computing
Vol. 2, No. 1 (2018)

Original research paper
UDC **519.852:621.316**
DOI **10.7251/IJEEC1801011M**

Power flow in radial distribution systems in the presence of harmonics

Miloš Milovanović[1], Jordan Radosavljević[1], Bojan Perović[1] and Milorad Dragičević[1]

[1] Faculty of Technical Sciences, University of Priština in Kosovska Mitrovica, Kosovska Mitrovica, Serbia

milos.milovanovic@pr.ac.rs, jordan.radosavljevic@pr.ac.rs, bojan.perovic@pr.ac.rs, dragicevicetf@gmail.com

Abstract—**This paper presents the results of power flow calculations in the presence of harmonics in radial distribution systems obtained using the decoupled harmonic power flow (DHPF) algorithm. In this algorithm, the interaction among the harmonic frequencies is assumed to be negligible and hence the calculations are separately performed for every harmonic order of interest. A detailed methodology for calculating current and voltage high order harmonics, harmonic losses and total harmonic distortion of voltage of the electrical distribution networks in the frequency domain is presented. The standard backward/forward sweep method is used for solving the power flow problem at the fundamental frequency. Furthermore, some practical and approximated models of network components in harmonic analysis are given. The performance of the DHPF approach is studied and evaluated on two standard test systems with nonlinear loads, the distorted IEEE 18-bus and IEEE 33-bus. Nonlinear loads are treated as harmonic current sources that inject harmonic currents into the system. The DHPF algorithm is verified by comparing its results with those generated by software tools for the analysis of transmission, distribution and industrial power systems (i.e. ETAP and PCFLO). Simulation results show the accuracy and efficiency of the applied procedure for solving the harmonic power flow problem.**

Keywords- decoupled approach; harmonic power flow; distribution system; nonlinear load

I. INTRODUCTION

In recent years, due to widespread usage of nonlinear loads, the distortion of the waveform of current and voltage increases. Loads with a nonlinear current-voltage characteristic inject a wide range of harmonics into the network, resulting in a deterioration of the power quality. These harmonics can cause various problems, such as the occurrence of series and parallel resonances, a reduction of efficiency in power generation, transmission and utilization, components ageing and capacity decrease, interferences with control devices and communication systems, etc. [1-3]. In general, the power flow calculation is carried out only for the fundamental frequency. However, in the power systems with nonlinear loads, the power flow calculation needs to be carried out for each harmonic frequency of interest. By including nonlinear loads into the calculation, the power flow calculation becomes more complex and demanding.

In scientific literature, different approaches have been proposed and implemented to solve the power flow problem in the presence of higher harmonics, named the harmonic power flow (HPF) [4-12]. The criteria to classify the harmonic power flow algorithms could be [2]: modeling technique for simulation of power system and nonlinear loads, system condition (single phase, three phase, balanced, unbalanced) and solution approaches.

Modeling techniques which are used for analyzing the harmonic problem include time domain [5], frequency domain [4], [6-12] and hybrid time-frequency domain [13]. Time domain approaches are based on transient analysis and have great flexibility and high accuracy. However, their use is limited because they usually require long computing time, especially for large power systems with many nonlinear loads. Frequency domain approaches calculate the frequency response of power systems and reduce the computation time of the scan process. The accuracy of the solution depends on the number of harmonics included in the calculation process. Hybrid approaches use a combination of frequency domain (to limit the computing time) and time domain (to increase the accuracy) approaches to simulate the power system and nonlinear loads, respectively. Based on their solution approaches, the harmonic power flow calculations can also be classified as coupled and decoupled methods [2].

Most nonlinear loads and power system components impose couplings between harmonics and call for accurate coupled solution approaches [2]. The coupled approach which is proposed in reference [6] solves simultaneously the calculation for all the harmonic orders and has good accuracy. The main disadvantages of this method are high computational costs and requirements for exact formulation of nonlinear loads. The decoupled approach [11,12] assumes that the coupling between harmonic orders can be rationally neglected and, as a result, the calculation can be separately carried out for every harmonic order. Therefore, this approach requires less computational costs [12].

This paper is a revised and expanded version of the paper presented at the XVII International Symposium INFOTEH-JAHORINA 2018 [22].

Correspondence to: M. Milovanović (milos.milovanovic@pr.ac.rs)

This paper presents the results of HPF calculations in radial distribution systems with nonlinear loads obtained using the decoupled harmonic power flow (DHPF) approach. The aim was to develop fast and efficient HPF algorithm that can easily be applied to other power system problems such as the problem of optimal placement and sizing of capacitor banks and/or distributed generators in radial distribution systems with nonlinear loads and the optimal filter design problem. The algorithm can be used to estimate the object function value of a considered optimization problem. The procedure is tested on two standard test systems with nonlinear loads, the distorted IEEE 18-bus and distorted IEEE 33-bus. To verify the accuracy of the DHPF approach, the simulation results are compared with those generated by software tools for the analysis of transmission, distribution and industrial power systems (i.e. ETAP [14] that uses the decoupled approach and PCFLO [15] that uses the coupled approach). Calculations showed the efficiency of the applied procedure for solving this complex problem.

II. MODELS FOR DISTRIBUTION NETWORK COMPONENTS

To analyze the industrial distribution systems, it is necessary to describe a detailed representation of component models such as distribution cables, transformers, shunt capacitors, reactors and loads. Instead of using the very accurate models, some practical and approximated models of [2], [9-12], [16] and [17] are used in this paper. At harmonic frequencies, a power system is modeled as a combination of passive elements and current sources that inject current into the power system. Fig. 1 shows an *m*-bus radial distribution system where a general bus *i* contains a load and a shunt capacitor.

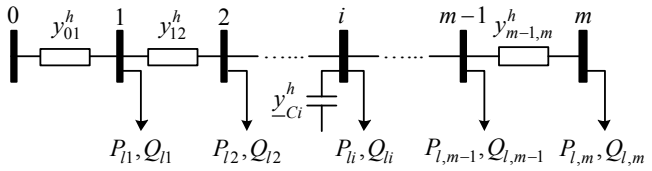

Figure 1. Single line diagram of a radial distribution system at harmonic frequencies [16]

A. Distribution lines and cables

The distribution lines and cables might be represented by the lumped parameter elements using a π-connection. If skin and proximity effects are ignored at higher frequencies, the longitudinal and shunt parameters of the lines are given by [9]

$$y_{\text{longitudinal}}^h = y_{i,i+1}^h = \frac{1}{R_{i,i+1} + j2\pi fhL_{i,i+1}}, \tag{1}$$

$$y_{\text{shunt}}^h = y_{i,i}^h = y_{i+1,i+1}^h = j2\pi fhC_{i,i+1}, \tag{2}$$

where $R_{i,i+1}$, $L_{i,i+1}$ and $C_{i,i+1}$, represent the resistance, inductance and capacitance of the line segment between busses *i* and *i*+1, respectively; *f* is the fundamental frequency of the system (*f*=50 Hz) and *h* is the harmonic order.

The skin effect can be included in (1) by modifying the resistive part of the line admittance as follows [9,17]:

$$R_{i,i+1}^h = R_{i,i+1}\left(1 + \frac{0.646h^2}{192 + 0.518h^2}\right), \tag{3}$$

$$R_{i,i+1}^h = R_{i,i+1}\left(0.187 + 0.532\sqrt{h}\right). \tag{4}$$

Equation (3) is for overhead lines and (4) for power cables.

B. Linear and nonlinear loads

Linear passive loads that do not produce harmonics have a significant effect on system frequency response primarily near resonant frequencies [17]. Linear loads are basically those loads that can be described as passive loads in terms of harmonics. At the fundamental frequency, linear loads are modeled as PQ buses while shunt admittances are used to model them at harmonic frequencies. Different types of linear load models at harmonic frequencies are recommended in the [17]. The choice of the load model to use depends on the nature of the load and on the information available. The generalized model is suggested for a linear load, which is composed by a resistance in parallel with a reactance. The admittance of the linear load connected at bus *i* is defined by [2], [9-12]

$$y_{li}^h = \frac{P_{li}}{\left|V_i^1\right|^2} - j\frac{Q_{li}}{h\left|V_i^1\right|^2}, \tag{5}$$

where P_{li} and Q_{li} are the active and reactive linear loads at bus *i*, respectively, and V_i^1 is the fundamental voltage at bus *i*.

Nonlinear loads are treated as decoupled harmonic current sources that inject harmonic currents into the system. The type of nonlinear loads is considered to be a three phase, six-pulse converter. Harmonics generated by converters of any pulse number can be expressed as [17]:

$$h = kq \pm 1, \tag{6}$$

where *k* is any integer (1,2,3,…, etc.) and *q* is the pulse number of the converter (6 in case of a six-pulse converter). According to the (6), it is obvious that the characteristic harmonics for a three phase, six-pulse converter are all odd harmonics except triplens (5th, 7th, 11th, etc.). The fundamental and the *h*th harmonic currents of the nonlinear load installed at bus *i* with fundamental real power P_{nl} and fundamental reactive power Q_{nl} are [2]

$$I_{nli}^1 = \left[\frac{P_{nli} + jQ_{nli}}{V_i^1}\right]^*, \tag{7}$$

$$I_{nli}^h = \frac{I_{nli}^1}{h}, \tag{8}$$

where I_{nli}^1 is the amplitude of the rms value of the fundamental current, I_{nli}^h the amplitude of the harmonic current of order *h* and * denotes the complex conjugate. According to [17], if there is a single source of harmonics in the system, then the phase angles of harmonic currents can be ignored.

C. Shunt capacitors

Shunt capacitors are represented as shunt connected elements:

$$y_{Ci}^h = hy_{Ci}^1, \tag{9}$$

where y_{Ci}^{1} is the admittance of shunt capacitor C at bus *i*.

III. DECOUPLED APPROACH FOR HARMONIC POWER FLOW

The method that is used to analyze and obtain the parameters of the distribution network at the fundamental harmonic is known as backward-forward sweep [18,19]. The power flow analysis at the fundamental frequency is the base for harmonic calculations. For the estimation of harmonic components, the DHPF method is used. In the decoupled method, the interaction among the harmonic frequencies is assumed to be negligible and hence the admittance matrix is formulated individually for all the higher order harmonic components. After modifying admittance matrix and associated harmonic currents, the HPF problem can be calculated using the equation [11]:

$$\mathbf{V^h} = \left(\mathbf{Y_{BUS}^h}\right)^{-1} \mathbf{I^h}, \tag{10}$$

where $\mathbf{Y_{BUS}^h}$ is the bus admittance matrix of the *h*th harmonic; $\mathbf{I^h} = \left[I_1^h, I_2^h, ..., I_n^h\right]^{\mathrm{T}}$ is the *h*th injected harmonic current vector and $\mathbf{V^h} = \left[V_1^h, V_2^h, ..., V_n^h\right]^{\mathrm{T}}$ is the *h*th harmonic voltage vector.

At any bus *i*, the rms value of the voltage and the total harmonic distortion of voltage (THD_V) are given by [11]

$$V_{rmsi} = \sqrt{\sum_{h=1}^{h_{\max}} \left|V_i^h\right|^2}, \tag{11}$$

$$THD_{Vi} = \frac{1}{\left|V_i^1\right|} \cdot \sqrt{\sum_{h\neq 1}^{h_{\max}} \left|V_i^h\right|^2} \times 100(\%), \tag{12}$$

where $h_{\max}$ is the maximum harmonic order under consideration.

Subsequently, superposition is applied to convert the solved values of each $\mathbf{V^h}$ into the time domain for each network bus *i* as follows [17]:

$$v_i(t) = \sum_{h=1}^{h_{\max}} V_i^h \sin\left(h\omega_1 t + \delta_i^h\right), \tag{13}$$

where $\omega_1 = 2\pi f$ is angular frequency and δ_i^h is the phase angle of the *h*th harmonic voltage.

At the *h*th harmonic frequency, the active power losses in the line section between bus *i* and *i*+1 are [11]:

$$P_{loss(i,i+1)}^h = R_{i,i+1}^h \left(\left|V_i^h - V_{i+1}^h\right| \left|y_{i,i+1}^h\right|\right)^2. \tag{14}$$

The total active power losses of the system for all harmonics are therefore given by the following equation [11]:

$$P_{loss}^h = \sum_{h=1}^{h_{\max}} \left(\sum_{i=0}^{m-1} P_{loss(i,i+1)}^h \right), \tag{15}$$

where *m* is the total number of buses. Similarly, the reactive power losses can be calculated but they have rarely been used in literature. The flow chart of the DHPF algorithm is shown in Fig. 2.

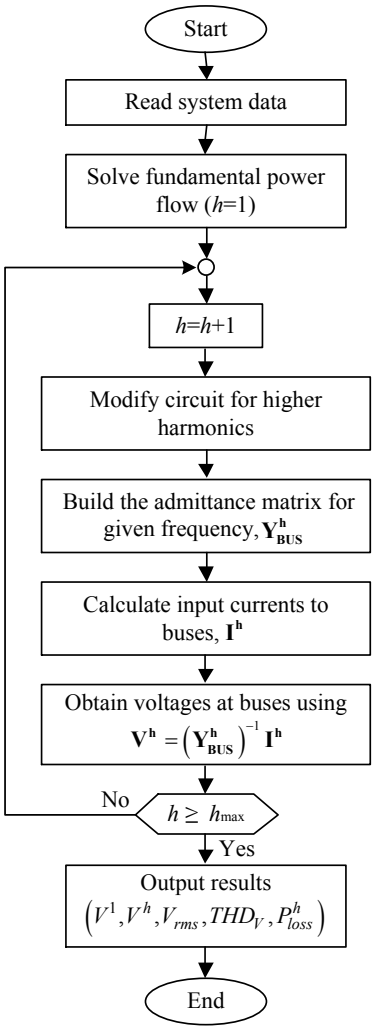

Figure 2. Flow chart of the DHPF algorithm

IV. RESULTS AND DISCUSSION

The proposed procedure is implemented in the MATLAB R2017b computing environment and run on a 2.70-GHz PC with 8 GB RAM. To reveal the validity of the DHPF algorithm, the IEEE 18-bus and IEEE 33-bus distorted radial distribution test systems are examined. The calculation includes harmonics up to the 49th harmonic.

A. Case 1

Fig. 3 shows a single line diagram of the 12.5 kV, IEEE 18-bus distorted radial distribution system. The substation voltage magnitude is set to 1.05 p.u. and it is assumed that the substation voltage does not contain any harmonic components. The parameters of the system are taken from [20] and given in Table A.I in the Appendix A. The base voltage for this system is 12.5 kV and base power is 10 MVA. The system contains a

six-pulse converter at bus 5 with active and reactive powers of 0.3 p.u. (3 MW) and 0.226 p.u. (2.26 MVAr), respectively. Current harmonic injections of the converter are calculated as fractions of the fundamental component using (8). Phase angles of harmonic currents are neglected since there is a single source of harmonics in the system [17]. At the fundamental frequency, the constant power model is used to model loads, while capacitor banks are modeled as constant admittances (impedances).

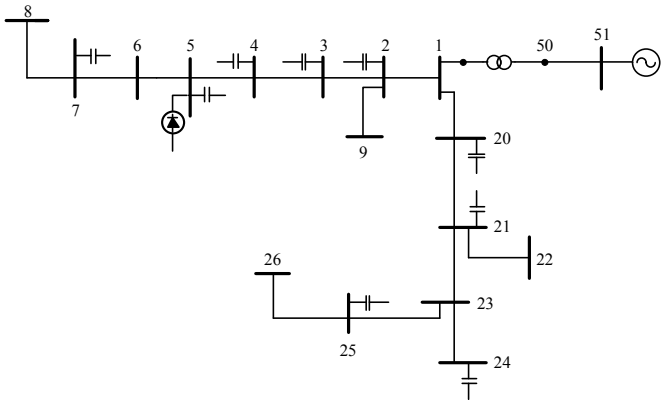

Figure 3. Single line diagram of the IEEE 18-bus test system

The generated results of the DHPF method and those generated by ETAP and PCFLO software packages including rms voltage and THD of voltage are shown in Figs. 4–6. Fig. 7 and Table B.I in the Appendix B show the harmonic voltage distortion versus frequency at all test system buses obtained using the DHPF.

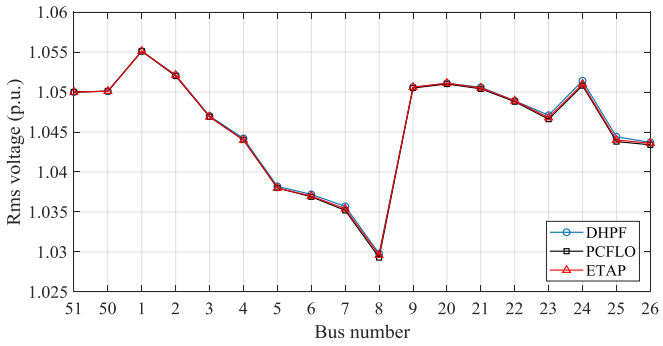

Figure 4. Rms voltage of the distorted IEEE 18-bus system generated by DHPF, PCFLO and ETAP

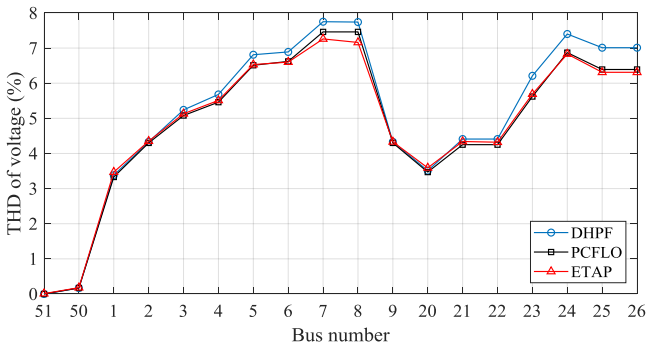

Figure 5. THD of voltage of the distorted IEEE 18-bus system generated by DHPF, PCFLO and ETAP

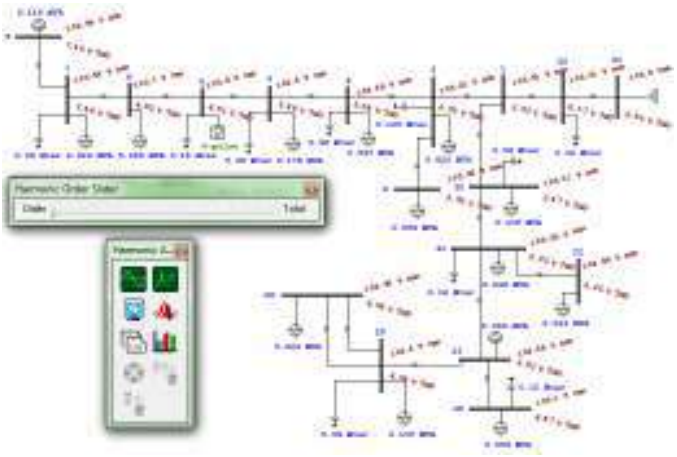

Figure 6. ETAP model of the IEEE-18 test system

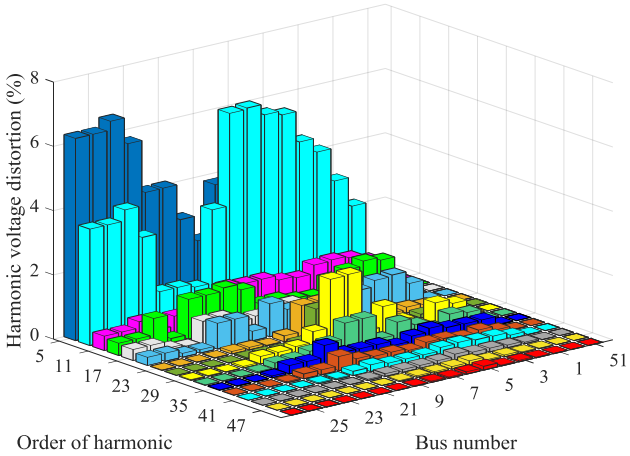

Figure 7. Voltage distortion versus frequency at all test system buses generated by DHPF

The deviations of results including the maximum and mean deviations generated by DHPF from those generated by PCFLO and ETAP are indicated in Table I. The main reason of the comparison is to demonstrate accuracy of the proposed DHPF algorithm.

TABLE I. THE MAXIMUM AND MEAN DEVIATIONS OF THE RESULTS FOR IEEE 18-BUS TEST SYSTEM

Results	Mean absolute deviation (%) with		Maximum deviation (%) with	
	PCFLO	ETAP	PCFLO	ETAP
V_{rms}	0.024	0.013	0.061	0.038
THD_V	4.144	4.579	10.413	11.068

From Table I, and from Figs. 4 and 5, it can be seen that the results of the DHPF algorithm and PCFLO and ETAP packages are very similar. There are some differences at some buses, mostly due to the neglected harmonic coupling by DHPF. In addition, the accuracy of the solution depends on method of modeling the elements of the system, and the impacts of skin effect and phase angles of harmonic currents.

Figs. 8 and 9 illustrate the active power losses for each line at the fundamental frequency and higher frequencies obtained using the DHPF method. The total active power losses of the system that are consist of the fundamental frequency component and the harmonic power caused by the presence of the converter are 279.450 kW. The average CPU time of the DHPF algorithm for IEEE 18-bus test system was 0.20 sec.

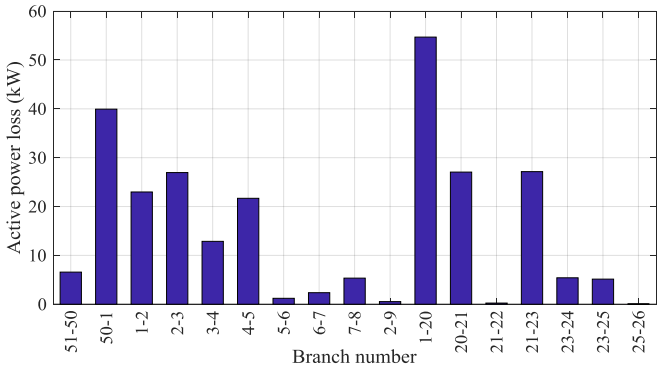

Figure 8. The active power losses at the various lines for the fundamental frequency in the IEEE 18-bus test system

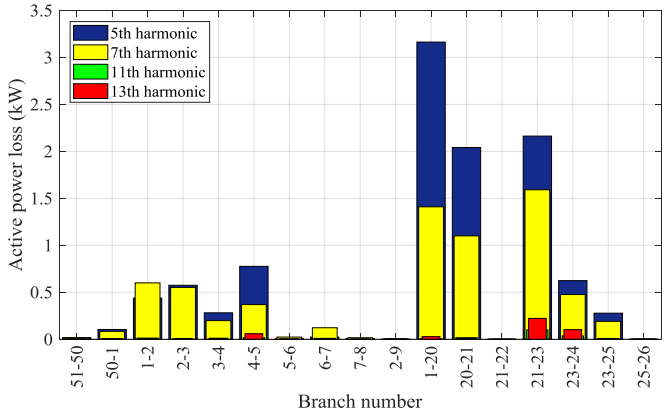

Figure 9. The active power losses at the various lines for 5th, 7th, 11th and 13th harmonic orders in the IEEE 18-bus test system

As could be expected, the losses at 5th and 7th orders are much higher than any others. Figs. 10 and 11 show the waveforms of voltage and current at the bus 5, respectively. Obviously, the waveform of voltage is not a pure sinusoidal waveform with only a 50 Hz frequency component.

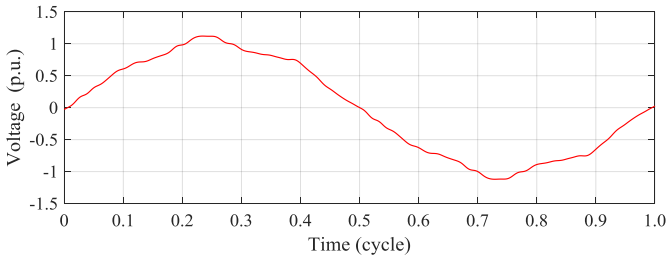

Figure 10. The voltage waveform at the bus 5

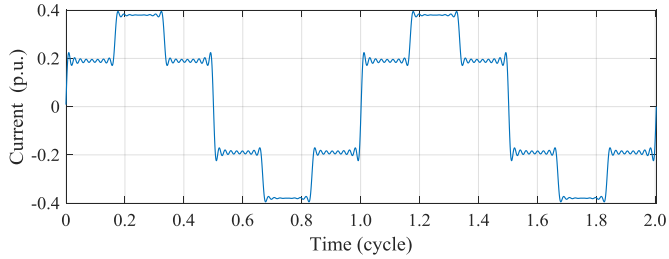

Figure 11. The nonsinusoidal current waveform of the six-pulse converter located at the bus 5

B. Case 2

To check the validity of the DHPF algorithm, the IEEE 33-bus radial distribution system [21] is considered. The base voltage and power of this system are 12.66 kV and 10 MVA, respectively. A single-line diagram of the system is shown in Fig. 12 and the details of loads and lines are listed in Table A.II in the Appendix A.

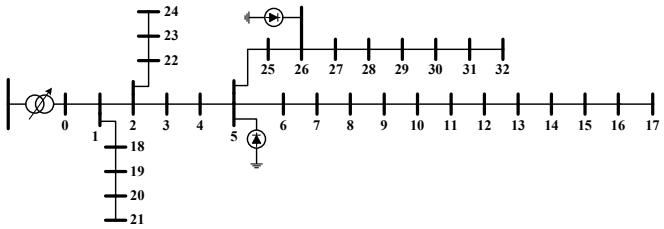

Figure 12. Single line diagram of the IEEE 33-bus test system

This system contains two three phase, six-pulse converters that are located at nodes 5 and 26 with active and reactive powers of 0.1 p.u. (1 MW) and 0.075 p.u. (0.75 MVAr), respectively. The nonsinusoidal current waveform of converters is the same as that in Fig. 11. The results that are generated by DHPF, PCFLO and ETAP are compared, as shown in Figs. 13 and 14. The THD of voltage, given in Fig. 14 and Table B.II in the Appendix B, shows the spreading of harmonic distortion among of buses due to the distributed nonlinear loads.

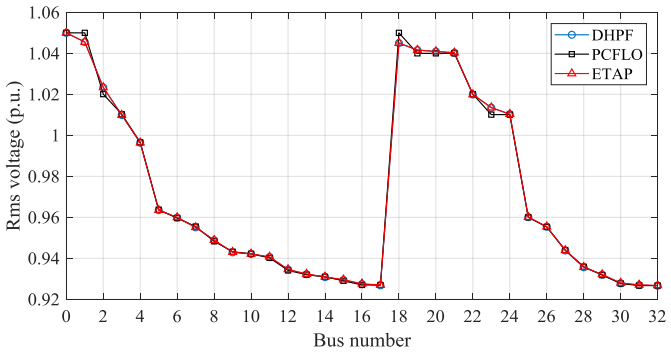

Figure 13. Rms voltage of the distorted IEEE 33-bus system generated by DHPF, PCFLO and ETAP

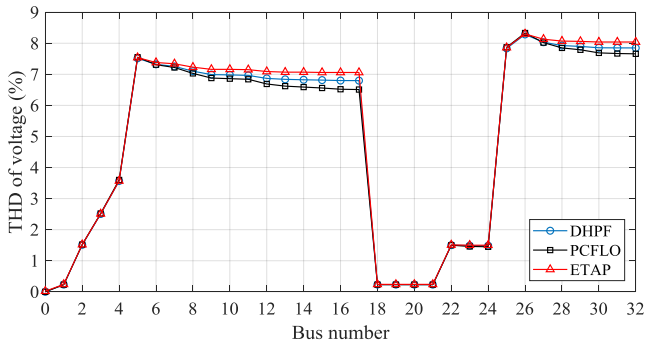

Figure 14. THD of voltage of the distorted IEEE 33-bus system generated by DHPF, PCFLO and ETAP

The maximum and mean deviations of the results are summarized in Table II.

TABLE II. THE MAXIMUM AND MEAN DEVIATIONS OF THE RESULTS FOR IEEE 33-BUS TEST SYSTEM

Results	Mean absolute deviation (%) with		Maximum deviation (%) with	
	PCFLO	ETAP	PCFLO	ETAP
V_{rms}	0.076	0.008	0.476	0.020
THD_V	1.578	2.031	4.415	3.954

The results from Table II, and Figs. 13 and 14, indicate the high compatibility of the results obtained by the DHPF procedure with those generated by PCFLO and ETAP software packages.

The fundamental frequency losses (Fig. 15) and harmonic losses (Fig. 16) of the system are 526.877 kW and 9.011 kW, respectively. Therefore, the total active power losses in the considered network are 535.888 kW.

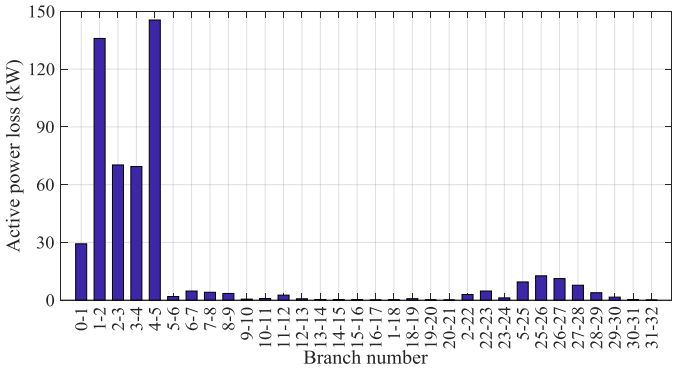

Figure 15. The active power losses at the various lines for the fundamental frequency in the IEEE 33-bus test system

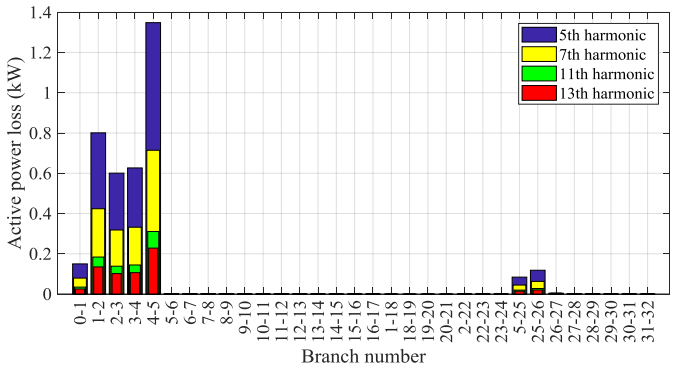

Figure 16. The active power losses at the various lines for the 5th, 7th, 11th and 13th harmonic orders in the IEEE 33-bus test system

The average CPU time of the DHPF algorithm for IEEE 33-bus test system was 0.25 sec.

V. CONCLUSION

In this paper, the application of decoupled approach for harmonic power flow in radial distribution systems with nonlinear loads is presented. The main conclusions that can be drawn from the presented results are:

- The DHPF algorithm for harmonic analysis of distribution systems allows quickly, easily and accurate calculation of the voltage and current harmonics, harmonic losses and the total harmonic distortion.
- Mean absolute deviations of results obtained by the DHPF algorithm from those generated by ETAP and PCFLO software packages are less than 5%. This means that the accuracy of the DHPF algorithm is high.
- The DHPF algorithm requires less CPU time and memory storage than ETAP and PCFLO.
- The solution can always be obtained directly, and it is computationally efficient.
- The decoupled approach can be applied to harmonic analysis of large distribution systems with multiple nonlinear loads.

ACKNOWLEDGMENT

This work was supported by the Ministry of Education, Science and Technological Development of the Republic of Serbia under research grant TR 33046.

REFERENCES

[1] N. Bayan, Harmonic flow analysis in power distribution networks, University of Windsor, Ontario, 1999.

[2] E. Fuchs and M. A. S. Masoum, Power quality in power systems and electrical machines, 1st ed., Elsevier, USA, 2008.

[3] J. Arrillaga and N. R Watson, Power system harmonics, 2nd ed., John Wiley & Sons, University of Canterbury, Christchurch, New Zealand, 2003.

[4] S. Herraiz, L. Sainz and J. Clua, "Review of harmonic load flow formulations," IEEE Trans. Power Syst., vol. 18, pp. 1079-1087, 2003.

[5] H. W. Dommel, Electromagnetic transients programs reference manual (EMTP Theory Book), Bonneville Power Administration Portland, 1986.

[6] D. Xia and G. T. Heydt, "Harmonic power flow studies part I – formulation and solution," IEEE Trans. Power Appar. Syst., vol. PAS-101, pp. 1257-1265, 1982.

[7] J. H. Teng and C. Y. Chang, "Backward/forward sweep based harmonic analysis method for distribution systems," IEEE Trans. Power Deli., vol. 22, pp. 1665–1672, 2007.

[8] I. Archundia-Aranda and R. O. Mota-Palomino, "Harmonic penetration method for radial distribution networks," International Journal of Emerging Electric Power Systems, vol. 15, pp. 111–117, 2014.

[9] D. Šošić, M. Žarković and G. Dobrić, "Fuzzy-based Monte Carlo simulation for harmonic load flow in distribution networks," IET Generation, Transmission & Distribution, vol. 9, pp. 267-275, 2015.

[10] M. Milovanović, J. Radosavljević and B. Perović, "Optimal location and sizing of capacitor banks in distribution networks to reduce harmonic distortion and improve voltage profile using genetic algorithm," Technics: Magazine of the Union of Engineers and Technicians of Serbia, ISSN 0013-5836, pp. 867-875, 2017.

[11] A.Ulinuha and M. A. S. Masoum, "Harmonic power flow calculations for a large power system with multiple nonlinear loads using decouple approach," in Australasian Universities Power Engineering Conference 2007. AUPEC 2007, pp. 1-6. 2007.

[12] A. Ulinuha, "Application of decouple approach for harmonic power flow calculation," Gelagar, 17 (2), pp. 83-90, 2006.

[13] M. A. Moreno López de Saá and J. Usaola Garcia, "Three-phase harmonic load flow in frequency and time domains," IEE Proc. – Electr. Power Appl., vol. 150, pp. 295-300, 2003.

[14] "ETAP user guide 12.6," Operation Technology, Inc, 2014.

[15] W. M. Grady, "PCFLO version 6.0 user manual," The University of Texas at Austin, 2011.

[16] Y. Baghzous and S. Ertem, "Shunt capacitor sizing for radial distribution feeders with distorted substation voltages," IEEE Trans. Power Delivery, vol. 5, pp. 650-657, 1990.

[17] A. Bonner, T. Grebe, E. Gunther, L. Hopkins, M. B. Marz, J. Mahseredjian, N. W. Miller, T. H. Omneyer, V. Rajagopalan, S. J. Ranade, P. F. Ribeiro, B. R. Shperling, T. R. Sims, W. Xu, "Modeling and simulation of the propagation of harmonics in electric power networks," Part I & II, IEEE Trans. Power Deli., vol. 11, no. 1, pp. 452-474, 1996.

[18] D. Shirmohammadi, H. W. Hong, A. Semlyen and G. X. Luo, "A compensation-based power flow method for weakly meshed distribution and transmission networks," IEEE Trans. Power Syst., vol. 3, pp. 753-762, 1988.

[19] C. S. Cheng and D. Shirmohammadi, "A three-phase power flow method for real-time distribution system analysis," IEEE Trans. Power Syst., vol. 10, pp. 671-679, 1995.

[20] W. M. Grady, M. J. Samotyj, and A. H. Noyola, "The application of network objective functions for actively minimizing the impact of voltage harmonics in power systems," IEEE Trans. Power Delivery, vol. 7, pp. 1379–1386, July 1992.

[21] S. Goswami and S. Basu, "A new algorithm for the reconfiguration of distribution feeders for loss minimization," IEEE Transactions on Power Delivery, vol. 7, pp. 1484-1491, July 1992.

[22] M. Milovanović, J. Radosavljević, B. Perović, M. Dragičević, "Power flow in radial distribution systems in the presence of higher harmonics," 17th International Symposium Infoteh-Jahorina, ISBN 978-99976-710-1-1, pp. 127–131, March 2018.

Miloš Milovanović was born in Serbia in 1991. He received the BSc and MSc degrees in electrical engineering and computer science from the Faculty of Technical Sciences, University of Priština, Kosovska Mitrovica, Serbia, in 2013 and 2015, respectively, and is currently pursuing the PhD degree in electrical engineering and computer science at the same faculty. His research interests include power system analysis, power quality and distributed power generation

Jordan Radosavljević was born in Serbia in 1973. He received his BSc degree in 1998 from the Faculty of Electrical Engineering, University of Priština, MSc degree in 2003 from the Faculty of Electrical Engineering, University of Belgrade and PhD degree in 2009 from the Faculty of Technical Sciences, Priština University in Kosovska Mitrovica. His main research interests include power system analysis, electric power distribution and distributed power generation.

Bojan Perović was born in Serbia in 1988. He received the BSc and MSc degrees in electrical engineering and computer science from the Faculty of Technical Sciences, University of Priština, Kosovska Mitrovica, Serbia, in 2011 and 2012, respectively, and is currently pursuing the PhD degree in electrical engineering and computer science at the same faculty. His research interests include renewable energy sources.

Milorad Dragičević was born in 1992 and he is a student currently pursuing the MSc degree in electrical engineering and computer science at the Faculty of Technical Sciences of University of Priština in Kosovska Mitrovica, Serbia. He received the BSc degree in electrical engineering and computer science at the same faculty in 2017. His research interests are in the field of electrical circuit analysis and power system analysis.

APPENDIX A

TABLE A.I. LINE DATA AND LOAD DATA FOR IEEE 18-BUS TEST SYSTEM*

Sending bus	Receiving bus	Section parameters			Linear load at receiving bus		Nonlinear load at receiving bus		Shunt load
		R (p.u.)	X (p.u.)	B (p.u.)	P_l (p.u.)	Q_l (p.u.)	P_{nl} (p.u.)	Q_{nl} (p.u.)	Q_C (p.u.)
1	2	0.00431	0.01204	0.000035	0.0200	0.0120	0.0000	0.0000	0.1050
2	3	0.00601	0.01677	0.000049	0.0400	0.0250	0.0000	0.0000	0.0600
3	4	0.00316	0.00882	0.000026	0.1500	0.0930	0.0000	0.0000	0.0600
4	5	0.00896	0.02502	0.000073	0.0000	0.0000	0.3000	0.2260	0.1800
5	6	0.00295	0.00824	0.000024	0.0800	0.0500	0.0000	0.0000	0.0000
6	7	0.01720	0.0212	0.000046	0.0200	0.0120	0.0000	0.0000	0.0600
7	8	0.04070	0.03053	0.000051	0.1000	0.0620	0.0000	0.0000	0.0000
2	9	0.01706	0.02209	0.000043	0.0500	0.0310	0.0000	0.0000	0.0000
1	20	0.02910	0.03768	0.000074	0.1000	0.0620	0.0000	0.0000	0.0600
20	21	0.02222	0.02877	0.000056	0.0300	0.0190	0.0000	0.0000	0.1200
21	22	0.04803	0.06218	0.000122	0.0200	0.0120	0.0000	0.0000	0.0000
21	23	0.03985	0.05160	0.000101	0.0800	0.0500	0.0000	0.0000	0.0000
23	24	0.02910	0.03768	0.000074	0.0500	0.0310	0.0000	0.0000	0.1500
23	25	0.03727	0.04593	0.000100	0.1000	0.0620	0.0000	0.0000	0.0900
25	26	0.02208	0.02720	0.000059	0.0200	0.0120	0.0000	0.0000	0.0000
25	26	0.02208	0.02720	0.000059	0.0000	0.0000	0.0000	0.0000	0.0000
1	50	0.00312	0.06753	0.000000	0.0000	0.0000	0.0000	0.0000	0.1200
50	51	0.00050	0.00344	0.000000	0.0000	0.0000	0.0000	0.0000	0.0000

* The values of the parameters and powers are given for the base values: 10 MVA and 12.5 kV.

TABLE A.II. LINE DATA AND LOAD DATA FOR IEEE 33-BUS TEST SYSTEM*

Sending bus	Receiving bus	Section parameters		Linear load at receiving bus		Nonlinear load at receiving bus	
		R (p.u.)	X (p.u.)	P_l (p.u.)	Q_l (p.u.)	P_{nl} (p.u.)	Q_{nl} (p.u.)
0	1	0.00575	0.00293	0.0100	0.0060	0.0000	0.0000
1	2	0.03076	0.01567	0.0090	0.0040	0.0000	0.0000
2	3	0.02284	0.01163	0.0120	0.0080	0.0000	0.0000
3	4	0.02378	0.01211	0.0060	0.0030	0.0000	0.0000
4	5	0.05110	0.04411	0.0060	0.0020	0.1000	0.0750
5	6	0.01168	0.03861	0.0200	0.0100	0.0000	0.0000
6	7	0.04439	0.01467	0.0200	0.0100	0.0000	0.0000
7	8	0.06426	0.04617	0.0060	0.0020	0.0000	0.0000
8	9	0.06514	0.04617	0.0060	0.0020	0.0000	0.0000
9	10	0.01227	0.00406	0.0045	0.0030	0.0000	0.0000
10	11	0.02336	0.00772	0.0060	0.0035	0.0000	0.0000
11	12	0.09159	0.07206	0.0060	0.0035	0.0000	0.0000
12	13	0.03379	0.04448	0.0120	0.0080	0.0000	0.0000
13	14	0.03687	0.03282	0.0060	0.0010	0.0000	0.0000
14	15	0.04656	0.03400	0.0060	0.0020	0.0000	0.0000
15	16	0.08042	0.10738	0.0060	0.0020	0.0000	0.0000
16	17	0.04567	0.03581	0.0090	0.0040	0.0000	0.0000
1	18	0.01023	0.00976	0.0090	0.0040	0.0000	0.0000
18	19	0.09385	0.08457	0.0090	0.0040	0.0000	0.0000
19	20	0.02555	0.02985	0.0090	0.0040	0.0000	0.0000
20	21	0.04423	0.05848	0.0090	0.0040	0.0000	0.0000
2	22	0.02815	0.01924	0.0090	0.0050	0.0000	0.0000
22	23	0.05603	0.04424	0.0420	0.0200	0.0000	0.0000
23	24	0.05590	0.04374	0.0420	0.0200	0.0000	0.0000
5	25	0.01267	0.00645	0.0060	0.0025	0.0000	0.0000
25	26	0.01773	0.00903	0.0060	0.0025	0.1000	0.0750
26	27	0.06607	0.05826	0.0060	0.0020	0.0000	0.0000
27	28	0.05018	0.04371	0.0120	0.0070	0.0000	0.0000
28	29	0.03166	0.01613	0.0200	0.0600	0.0000	0.0000
29	30	0.06080	0.06008	0.0150	0.0070	0.0000	0.0000
30	31	0.01937	0.02258	0.0210	0.0100	0.0000	0.0000
31	32	0.02128	0.03308	0.0060	0.0040	0.0000	0.0000

* The values of the parameters and powers are given for the base values: 10 MVA and 12.66 kV.

APPENDIX B

TABLE B.I. HARMONIC VOLTAGE DISTORTIONS AND THD OF THE DISTORTED IEEE 18-BUS SYSTEM

Bus number	**Voltage distortion (%) of each harmonic**																***THD*$_V$ (%)**
	5	**7**	**11**	**13**	**17**	**19**	**23**	**25**	**29**	**31**	**35**	**37**	**41**	**43**	**47**	**49**	
51	0.00	0.00	0.00	0.00	0.00	0.00	0.00	0.00	0.00	0.00	0.00	0.00	0.00	0.00	0.00	0.00	0.00
50	0.09	0.11	0.04	0.05	0.01	0.03	0.01	0.00	0.03	0.02	0.02	0.01	0.01	0.01	0.00	0.00	0.17
1	1.87	2.30	0.86	1.00	0.25	0.61	0.12	0.08	0.46	0.33	0.26	0.12	0.11	0.05	0.02	0.01	3.38
2	2.11	3.17	1.05	1.10	0.46	0.98	0.17	0.11	0.59	0.41	0.27	0.23	0.20	0.08	0.03	0.02	4.33
3	2.54	4.17	1.11	0.96	0.57	0.94	0.10	0.05	0.06	0.12	0.28	0.14	0.21	0.11	0.06	0.04	5.24
4	2.80	4.61	1.08	0.81	0.55	0.76	0.04	0.01	0.34	0.34	0.38	0.22	0.26	0.12	0.04	0.03	5.68
5	3.59	5.58	0.83	0.43	0.34	0.30	0.18	0.14	0.86	0.54	0.27	0.24	0.23	0.18	0.13	0.11	6.81
6	3.63	5.71	0.89	0.47	0.42	0.41	0.38	0.29	0.25	0.17	0.13	0.12	0.13	0.11	0.08	0.07	6.89
7	3.73	6.05	1.03	0.59	0.63	0.71	0.98	1.02	2.08	0.90	0.26	0.19	0.13	0.09	0.05	0.04	7.75
8	3.73	6.04	1.03	0.59	0.63	0.70	0.97	1.02	2.07	0.89	0.26	0.18	0.13	0.09	0.05	0.04	7.74
9	2.11	3.17	1.05	1.10	0.46	0.98	0.17	0.11	0.59	0.41	0.27	0.23	0.20	0.08	0.03	0.02	4.33
20	2.86	1.00	0.75	1.27	0.42	0.28	0.02	0.02	0.27	0.28	0.60	0.42	0.13	0.04	0.01	0.01	3.51
21	3.91	1.11	0.53	1.18	0.67	0.76	0.08	0.04	0.22	0.18	0.25	0.15	0.03	0.01	0.00	0.00	4.41
22	3.91	1.11	0.53	1.18	0.67	0.77	0.08	0.04	0.22	0.18	0.25	0.15	0.03	0.01	0.00	0.00	4.41
23	5.50	2.85	0.24	0.14	0.06	0.10	0.01	0.01	0.05	0.04	0.06	0.04	0.01	0.00	0.00	0.00	6.20
24	6.27	3.78	0.61	0.86	0.13	0.12	0.01	0.00	0.02	0.01	0.01	0.01	0.00	0.00	0.00	0.00	7.40
25	6.04	3.48	0.43	0.37	0.33	0.24	0.01	0.01	0.02	0.02	0.02	0.01	0.00	0.00	0.00	0.00	7.01
26	6.04	3.48	0.43	0.37	0.33	0.24	0.01	0.01	0.02	0.02	0.02	0.01	0.00	0.00	0.00	0.00	7.01

TABLE B.II. HARMONIC VOLTAGE DISTORTIONS AND THD OF THE DISTORTED IEEE 33-BUS SYSTEM

Bus number	**Voltage distortion (%) of each harmonic**																***THD*$_V$ (%)**
	5	**7**	**11**	**13**	**17**	**19**	**23**	**25**	**29**	**31**	**35**	**37**	**41**	**43**	**47**	**49**	
0	0.00	0.00	0.00	0.00	0.00	0.00	0.00	0.00	0.00	0.00	0.00	0.00	0.00	0.00	0.00	0.00	0.00
1	0.07	0.07	0.07	0.07	0.06	0.06	0.06	0.06	0.05	0.05	0.05	0.05	0.05	0.05	0.05	0.04	0.23
2	0.49	0.46	0.44	0.43	0.41	0.40	0.38	0.37	0.35	0.35	0.33	0.32	0.31	0.30	0.29	0.29	1.50
3	0.80	0.77	0.73	0.71	0.68	0.66	0.63	0.61	0.59	0.57	0.55	0.54	0.52	0.51	0.49	0.48	2.49
4	1.14	1.09	1.03	1.01	0.96	0.94	0.90	0.88	0.84	0.82	0.78	0.77	0.74	0.72	0.70	0.69	3.54
5	2.35	2.27	2.17	2.12	2.03	1.99	1.90	1.86	1.77	1.74	1.67	1.63	1.57	1.54	1.49	1.47	7.47
6	2.34	2.26	2.16	2.11	2.00	1.95	1.85	1.81	1.71	1.67	1.59	1.55	1.48	1.45	1.39	1.36	7.28
7	2.34	2.26	2.15	2.10	1.99	1.94	1.84	1.79	1.69	1.65	1.56	1.52	1.45	1.42	1.36	1.33	7.21
8	2.34	2.26	2.14	2.08	1.97	1.91	1.80	1.75	1.64	1.60	1.50	1.46	1.38	1.34	1.28	1.24	7.06
9	2.34	2.25	2.13	2.07	1.95	1.89	1.77	1.72	1.61	1.56	1.46	1.41	1.33	1.29	1.22	1.18	6.95
10	2.34	2.25	2.13	2.07	1.95	1.89	1.77	1.71	1.61	1.55	1.46	1.41	1.33	1.29	1.21	1.18	6.94
11	2.34	2.25	2.13	2.07	1.95	1.89	1.77	1.71	1.60	1.55	1.45	1.40	1.32	1.28	1.20	1.17	6.92
12	2.34	2.25	2.12	2.06	1.93	1.87	1.74	1.68	1.57	1.51	1.41	1.36	1.27	1.23	1.15	1.12	6.83
13	2.33	2.25	2.12	2.05	1.93	1.86	1.74	1.68	1.56	1.50	1.40	1.35	1.26	1.22	1.14	1.10	6.80
14	2.33	2.25	2.12	2.05	1.92	1.86	1.73	1.67	1.55	1.50	1.39	1.34	1.25	1.21	1.13	1.09	6.79
15	2.33	2.25	2.11	2.05	1.92	1.86	1.73	1.67	1.55	1.49	1.39	1.34	1.25	1.20	1.12	1.09	6.77
16	2.33	2.25	2.11	2.05	1.92	1.85	1.73	1.66	1.55	1.49	1.38	1.33	1.24	1.20	1.12	1.08	6.76
17	2.33	2.24	2.11	2.05	1.92	1.85	1.73	1.66	1.54	1.49	1.38	1.33	1.24	1.20	1.12	1.08	6.76
18	0.07	0.07	0.07	0.07	0.06	0.06	0.06	0.06	0.05	0.05	0.05	0.05	0.05	0.05	0.05	0.04	0.23
19	0.07	0.07	0.07	0.07	0.06	0.06	0.06	0.06	0.05	0.05	0.05	0.05	0.05	0.05	0.04	0.04	0.23
20	0.07	0.07	0.07	0.07	0.06	0.06	0.06	0.06	0.05	0.05	0.05	0.05	0.05	0.05	0.04	0.04	0.23
21	0.07	0.07	0.07	0.07	0.06	0.06	0.06	0.06	0.05	0.05	0.05	0.05	0.05	0.05	0.04	0.04	0.23
22	0.48	0.46	0.44	0.43	0.41	0.40	0.38	0.37	0.35	0.34	0.33	0.32	0.31	0.30	0.29	0.28	1.49
23	0.48	0.46	0.44	0.43	0.41	0.39	0.37	0.36	0.35	0.34	0.32	0.31	0.30	0.29	0.28	0.27	1.48
24	0.48	0.46	0.44	0.43	0.40	0.39	0.37	0.36	0.35	0.34	0.32	0.31	0.30	0.29	0.28	0.27	1.47
25	2.45	2.37	2.26	2.21	2.12	2.07	1.98	1.93	1.85	1.81	1.74	1.70	1.64	1.61	1.55	1.53	7.79
26	2.59	2.50	2.39	2.34	2.24	2.19	2.09	2.05	1.96	1.91	1.84	1.80	1.73	1.70	1.64	1.62	8.24
27	2.58	2.49	2.37	2.32	2.20	2.15	2.04	1.98	1.88	1.83	1.74	1.70	1.62	1.58	1.51	1.47	7.99
28	2.58	2.49	2.37	2.31	2.19	2.13	2.01	1.96	1.85	1.80	1.70	1.65	1.56	1.52	1.45	1.41	7.88
29	2.58	2.49	2.36	2.30	2.18	2.12	2.01	1.95	1.84	1.79	1.69	1.64	1.55	1.51	1.43	1.40	7.85
30	2.58	2.49	2.36	2.30	2.18	2.12	2.00	1.94	1.83	1.77	1.67	1.62	1.53	1.49	1.41	1.37	7.81
31	2.58	2.49	2.36	2.30	2.18	2.11	1.99	1.94	1.82	1.77	1.67	1.62	1.53	1.49	1.41	1.37	7.81
32	2.58	2.49	2.36	2.30	2.18	2.11	1.99	1.94	1.82	1.77	1.67	1.62	1.53	1.49	1.41	1.37	7.81